THE JOURNAL OF PHYSICAL CHEMISTRY C
A JOURNAL OF THE AMERICAN CHEMICAL SOCIETY

pubs.acs.org/JPCC

Article

Coupling Silver Iodide Emitters to Aluminum Plasmons

Razieh Talebi,* Harald Ditlbacher, Joachim R. Krenn, and Andreas Hohenau

Cite This: https://dx.doi.org/10.1021/acs.jpcc.0c09025

Read Online

ACCESS | Metrics & More | Article Recommendations | Supporting Information

ABSTRACT: Silver iodide (AgI) is an efficient blue emitter that is easily synthesized and nanostructured. We investigate the coupling of AgI to plasmon modes, choosing aluminum (Al) owing to its low damping in the blue spectral range, in contrast to silver or gold. We investigate, first, an extended Al thin film overcoated with a SiO_2 spacer layer and a AgI film. Spectroscopic surface plasmon resonance measurements confirm the anticrossing in the system's dispersion diagram, with a large energy splitting of about 140 meV, indicative of the onset of strong coupling. Second, we probe Al nanodisks overcoated with SiO_2 and AgI, spectrally shifting the dipolar Al plasmon over the AgI absorption line by lithographically controlling the disk diameter. From extinction spectra, we again observe anticrossing, with an energy splitting of about 100 meV. Our results demonstrate that AgI is an easily fabricated and structured emitter, which in combination with Al forms an attractive platform to achieve an efficient plasmon−exciton coupling in the blue spectral range.

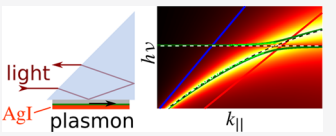

INTRODUCTION

The coupling of light emitters and plasmon modes leads to a vast range of effects, from the modification of absorption and emission rates, emission statistics, and emission profiles[1−3] to strong coupling.[4,5] In particular, strong coupling has attracted significant attention in recent years, involving mainly molecules[6,7] or semiconductor quantum dots.[8,9] Although most approaches have relied on the classical plasmonic materials such as silver and gold, some studies that focused on low-wavelength emitters have turned to aluminum (Al) owing to its low loss in the blue spectral range.[10,11] In this work, we show that silver iodide (AgI) is an efficient blue emitter that can be conveniently tailored to a target geometry by iodizing silver structures. We couple AgI to Al plasmons, evidencing the onset of strong coupling.

AgI, well known from early photography,[12] shows narrow absorption and emission features at room temperature, with a band edge slightly below 3 eV. Fabricated by the iodization of silver, the gradual change from the plasmonic (silver) to the excitonic (AgI) behavior has been probed spectroscopically.[13] The combination of AgI and plasmons has however been addressed in just a few studies, including spherical silver nanoparticles, where coupling leads to Fano lineshapes in absorbance spectra.[14] On the other hand, the plasmon peaks of gold nanoparticles were found to just experience spectral shifts due to the presence of AgI, due to the significant energy difference of gold plasmons and AgI absorption.[15]

Here, we couple AgI to the surface plasmons of Al in two different systems. We investigate, first, a thin AgI layer that is deposited onto an Al thin film covered with a SiO_2 spacer layer. Second, we probe the regular arrays of Al nanodisks covered with SiO_2 and AgI. The nanodisk diameter is varied, thus gradually changing the resonance positions of the Al localized surface plasmon resonance (LSPR). We observe clear coupling signatures in optical spectra that fit very well to simulations, based on the transfer matrix approach and a simple coupled oscillator model. In particular, we find a large energy splitting of about 140 meV in the thin film system, corresponding to the onset of strong coupling.

MATERIALS AND METHODS

Silver Iodide. AgI is a wide-gap semiconductor prepared by iodizing a silver thin film either structured or unstructured. For spectroscopic characterization, silver (island) films with 2 and 5 nm mass thicknesses are evaporated onto a quartz substrate by physical vapor deposition at about 5×10^{-6} mbar base pressure. The films are then exposed to the iodine vapor from a 5 mm-sized solid iodine crystal at about 4 cm distance at room temperature and ambient pressure for 10 min. The conversion of the Ag cubic phase to the AgI wurtzite phase (β-AgI) leads to a 4× volume enhancement[16] and thus nominal average AgI thicknesses of about 8 and 20 nm, respectively, as confirmed by an atomic force microscope. The films are basically discontinuous (on a 10 nm scale), reflecting the island characteristic of the silver thin films.

Optical absorbance spectra of AgI thin films with thicknesses of 8 and 20 nm on quartz plates are depicted in Figure 1a. The spectra indicate a sharp excitonic peak ($W_{1,2}$) at 2.94 eV and a small excitonic peak (W_3, not shown) at 3.77 eV.[17] The direct band gap of AgI thin films is determined by a Tauc plot,[17] yielding a value of 2.85 eV for both film thicknesses. The Tauc plot of AgI thin films is shown in Figure S1 in the Supporting Information.

Received: October 5, 2020
Revised: January 12, 2021

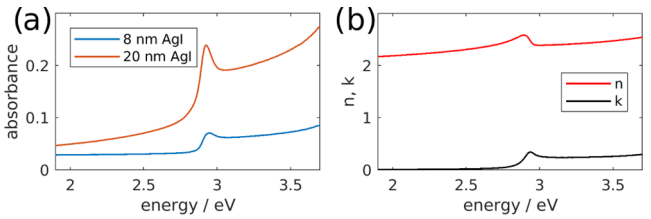

Figure 1. (a) Absorbance spectra of AgI layers on a quartz substrate, with thicknesses of 8 nm (blue) and 20 nm (orange). (b) Real (n, red) and imaginary parts (k, black) of the dielectric function of AgI as derived from (a).

The dielectric function of AgI was derived from the absorbance measurements on 8 and 20 nm thick AgI films. The derivation of the dielectric function is explained in the Supporting Information (see also Figure S2). The dielectric permittivity was presumed to be a sum of Lorentzian terms, whose amplitudes were adjusted to fit the simulated absorbance spectra, as calculated by the transfer matrix formalism (see below) to the experimental data (Figure 1a). The derived refractive index in Figure 1b is close to the published values.[18]

Preparation of Extended Al−SiO_2−AgI Films. A 20 nm thick Al thin film is evaporated onto a quartz substrate. The Al thickness is chosen for efficient surface plasmon excitation in the blue spectral range.[19] To avoid chemical reactions between Al and iodine and to prevent emitter quenching, a protective layer of 10 nm SiO_2 is evaporated onto the Al thin film. Then, a thin layer of Ag (2 or 5 nm mass thickness) is evaporated and iodized as described above. The mass thicknesses of the resulting AgI layers are 8 and 20 nm.

Fabrication of SiO_2−AgI-Covered Al Nanodisk Arrays. Arrays of disk-shaped Al nanoparticles were fabricated by electron beam lithography on an indium tin oxide (ITO)-coated glass substrate. First, a 100 nm thick layer of poly(methyl methacrylate) (PMMA) resist (Allresist ARP 671.01) is spin-coated onto the substrate and annealed for 15 min at 180 °C (Figure 2a). The resist is exposed by the

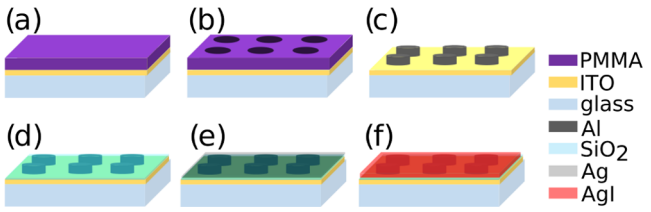

Figure 2. Electron beam lithography of Al−SiO_2−AgI nanodisks. (a) PMMA coating of the ITO-covered glass substrate, (b) electron beam exposure and development, (c) Al deposition and PMMA liftoff, (d) SiO_2 spacer layer deposition, (e) Ag evaporation, and (f) Ag iodization.

electron beam in a RAITH eLiNE+ lithography system. The applied pattern consists of circular holes with diameters ranging from about 50 to 90 nm, arranged in a quadratic array with a 200 nm pitch. The area of each array is 100 × 100 μm^2. After exposure, the samples are chemically developed (30 s Allresist ARP 600-55 mixed 2:1 with IPA, 30 s stopper Allresist ARP 600-60). Subsequently, 20 nm Al is evaporated by physical vapor deposition. Following 10 nm of SiO_2, 3.5 nm Ag is deposited and iodized, forming a AgI layer of about 14 nm mass thickness. Finally, the residual resist is removed by liftoff in acetone (Figure 2b−f).

SPR Spectroscopy. The plasmon-emitter coupling in the Al−SiO_2−AgI film system is measured by surface plasmon resonance (SPR) spectroscopy in the Kretschmann−Raether prism coupling configuration (see Figure 3a). Light reflection

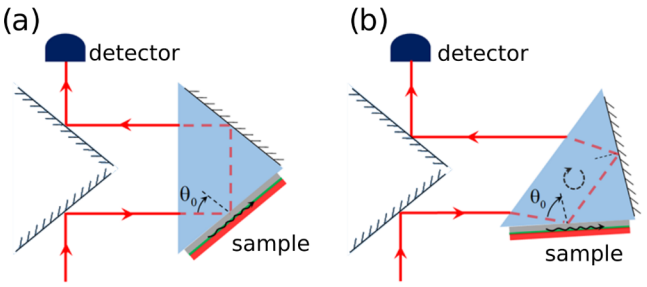

Figure 3. Sketch of the SPR setup with a rotating prism, for about (a) θ_0 = 45° and (b) θ_0 = 80°.

is measured for varying incident angles, controlled by the rotation of the prism supporting the sample (Figure 3b). The whole setup is placed inside a spectrophotometer (Varian Cary 5E) and reflection spectra are recorded for incidence angles θ_0 ranging from 45° to about 80°. The total internal reflection of the bare prism was used as reference for a reflectivity of 1. From the recorded spectra, we deduced the reflectivity as a function of photon energy and in-plane wavenumber, $k = nk_0 \sin\theta_0$, where k_0 is the vacuum wavenumber and n is the refractive index of the prism.

Optical Extinction Spectroscopy. The optical extinction of the covered Al nanodisk arrays is deduced from transmission spectra acquired with a spectrophotometer (Zeiss MMS1) fiber-coupled to an optical microscope (Zeiss Axioskop, objective 2.5×, numerical aperture 0.075) that is equipped with a halogen lamp. The useable spectral range is 400−1100 nm with a spectral resolution of about 3 nm.

Transfer Matrix Simulations. SPR spectra are calculated by a standard transfer matrix formalism with light incident from a SiO_2 (n = 1.46) half space. Then, layers of 20 nm Al (dielectric function from ref 10, 20), 10 nm SiO_2 (n = 1.46), and 8 nm or 20 nm AgI (for dielectric function, see Figure 1b) followed by an air half space (n = 1) are simulated. Further simulation schemes are discussed below.

RESULTS AND DISCUSSION

We first turn to the film system to investigate the coupling between surface plasmons at the Al−SiO_2 interface and excitons in 8 and 20 nm thick AgI layers. The thicker the AgI layer, the higher is the number of excitable AgI nanocrystals and thus stronger coupling is expected.

In Figure 4a,b, the measured reflectivity as a function of photon energy and in-plane wavenumber k are plotted for the AgI thicknesses of 8 and 20 nm, respectively. The corresponding transfer matrix simulations are shown in Figure 4c,d. The cyan dots in all figures indicate the reflection minima of the experimental data, determined by searching the corresponding reflection minimum for a fixed angle of incidence. We find excellent agreement between the experiment and simulation and observe a clear anticrossing[21−23] between the surface plasmon dispersion and the AgI resonance at 2.94 eV. The experimentally recorded, angle-dependent

https://dx.doi.org/10.1021/acs.jpcc.0c09025
J. Phys. Chem. C XXXX, XXX, XXX−XXX

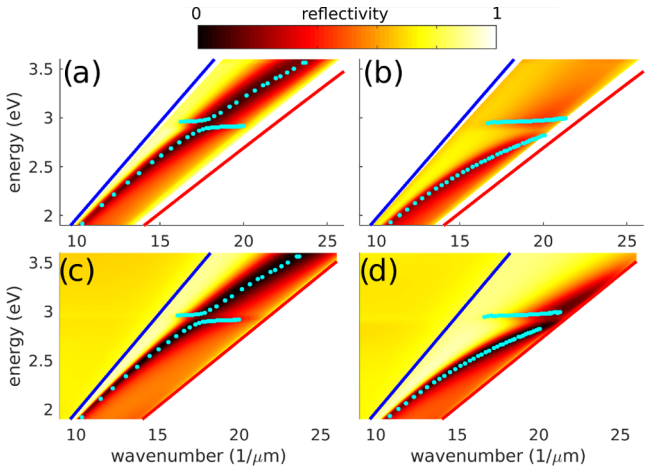

Figure 4. (a, b) Measured and (c, d) simulated reflection diagrams of an Al−SiO_2−AgI layer system with (a, c) 8 nm and (b, d) 20 nm AgI thicknesses. The cyan dots give the reflection minima as derived from the experimental data. The blue and red lines indicate the light lines in the air and the quartz substrate, respectively. In (b) and (d), only part of the anticrossing region can be observed. Due to the high refractive index of AgI, the surface plasmon dispersion is shifted to larger k-values, thus preventing coupling to light at wavenumbers close to and right of the red line.

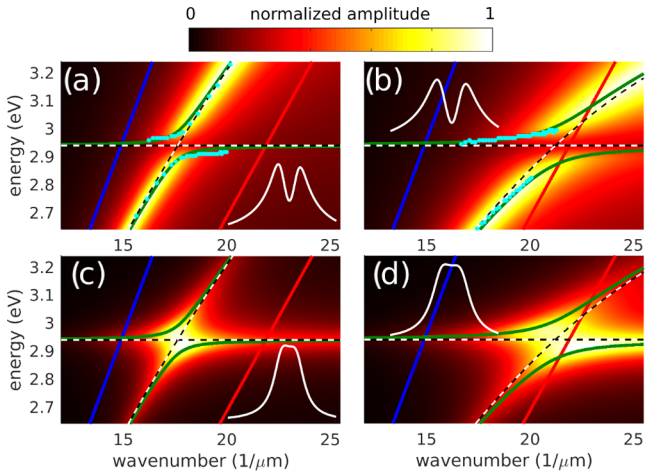

Figure 5. Model calculations of a system of two coupled oscillators. (a, b) Amplitude of the surface plasmon oscillator and (c, d) amplitude of the AgI oscillator, corresponding to Al−SiO_2−AgI layer systems with (a, c) 8 nm AgI and (b, d) 20 nm AgI thicknesses. The dashed black/white lines indicate the dispersion relations of the uncoupled oscillators. The green curves show the calculated resonance positions of the coupled system. The cyan dots indicate the experimental reflection minima, as shown in Figure 4. The blue and red lines are the light lines in air and the quartz substrate, respectively. The insets depict the energy dependence of the oscillator amplitudes at wavenumbers of (a, c) 17.6 μm^{-1} and (b, d) 21.2 μm^{-1}, respectively.

reflection spectra that were used to derive Figure 4a,b are shown in the Supporting Information (Figure S3).

For a better understanding of the coupling, we now model the experimental results by a simple system of two coupled, damped classical oscillators,[23] corresponding to the excitonic AgI resonance with fixed resonance energy and to the surface plasmon resonance of the Al layer. For the latter, the resonance energy is described as a function of the in-plane wavenumber, approximated by fitting a third-order polynomial to the experimental reflection minima, excluding the energy region of the AgI exciton around 2.9 eV. When neglecting the losses, the resonance energies of the system of coupled oscillators can be analytically described as[22−24]

$$\omega_{U,L}^2 = \frac{1}{2}(\omega_1^2 + \omega_2^2) \pm \frac{1}{2}\sqrt{(\omega_1^2 + \omega_2^2)^2 + 4\Gamma^2\omega_1\omega_2} \quad (1)$$

where ω_1 and ω_2 are the resonance energies of the uncoupled oscillators representing the AgI exciton (index 1) and the surface plasmon resonance (index 2) and Γ describes the (AgI thickness-dependent) energy splitting. However, here the oscillators are strongly damped and, as detailed below, this relation only describes roughly the observed resonances.

With Γ fitted to the experimental data, the dispersions (as noted, for the lossless case) are plotted as the green curves in Figure 5 for the layer systems with (a,c) 8 nm and (b,d) 20 nm AgI thicknesses. For comparison, the black/white dashed lines display the uncoupled oscillators. The green curves perfectly follow the experimental reflection minima (taken from Figure 4), plotted by the cyan dots, indicating that the plasmon−AgI coupling is very well described by the simple oscillator model. We deduce energy splittings of about 100 and 140 meV for the AgI thicknesses of 8 and 20 nm, respectively.

Despite the rather large energy splitting, we analyze our data further, as great care is advisable for plasmonic systems when claiming strong coupling, as illustrated in recent studies.[9,25,26] First, we deduce the spectral widths of the surface plasmon and the AgI at resonance, as outlined in Figures S4 and S5a. For the plasmon, we analyze the reflection data in Figure 4 and extrapolate a fit to the off-resonance width data to the resonance position. We find about 190 and 200 meV for the plasmon in the Al film covered with 8 and 20 nm AgI, respectively, and 60 nm for the AgI. Applying the threshold criterion according to ref 4 yields an energy value slightly above 140 meV, so that we conclude that the sample with 20 nm AgI is at the onset of strong coupling.

Then, we display separately the amplitudes of the plasmon and the AgI oscillators as simulated with losses included, see the color plots in Figure 5a,c (8 nm AgI) and Figure 5b,d (20 nm AgI). For both AgI thicknesses, the splitting of the plasmon oscillator into upper and lower energy branches is evident (Figure 5a,b and insets), with maxima well described by the green curves. However, the AgI oscillator amplitudes in Figure 5c,d display only weak energy splitting (AgI thickness 20 nm, Figure 5d). Here, despite the large splitting value, strong coupling is hampered by the relatively large damping of the AgI and the surface plasmon oscillator with a photon energy of 2.9 eV.

In more physical terms, it is the surface plasmon that is directly and strongly excited by light in the SPR geometry. The surface plasmon efficiently excites the AgI to high amplitude (in the oscillator model) and absorption around its resonance energy, in turn (corresponding to the weak coupling limit) leading to stronger damping and thus reducing the plasmon amplitude. The AgI oscillator thus has a stronger or even the largest amplitude at the resonance of the surface plasmon oscillator. The amplitude of the latter is, however, reduced due to the energy lost by driving the AgI. This leads to a more obvious splitting of the surface plasmon dispersion as compared to the AgI dispersion. Only with increasing coupling strength, a clear branch splitting is observed for both

https://dx.doi.org/10.1021/acs.jpcc.0c09025
J. Phys. Chem. C XXXX, XXX, XXX−XXX

oscillators. In Figure 5c) (inset), we observe just a shallow minimum between the amplitude peaks of upper and lower branches, while in Figure 5d (inset) this minimum is somewhat more pronounced. We thus conclude that we observe the onset of strong coupling and that optimized samples could operate in this regime, as there is a strong dependence of the energy splitting on SiO_2 and AgI thickness (Figure S6).

With larger splitting, the strongest excitation of AgI by the plasmon shifts further away from the AgI resonance energy; thus, the AgI splitting gets larger as well. It is expected to reach the values of the plasmon oscillator for even larger coupling strength. To clarify this, Figure S7 depicts the calculated energy splitting of the two coupled oscillators with different damping values (similar to the surface plasmon and AgI) as a function of coupling strength.

We now turn to the coupling of AgI and Al nanodisk LSPRs. The Al nanodisks have diameters of about 50−90 nm and heights of 20 nm Al, 10 nm SiO_2, and 13.5 nm AgI. The disk diameter tunes the spectral position of the LSPR, which was chosen to overlap with the AgI $W_{1,2}$ exciton peak. The measured diameter-dependent extinction spectra are depicted in Figure 6a,b. With increasing disk diameter, the LSPR peak

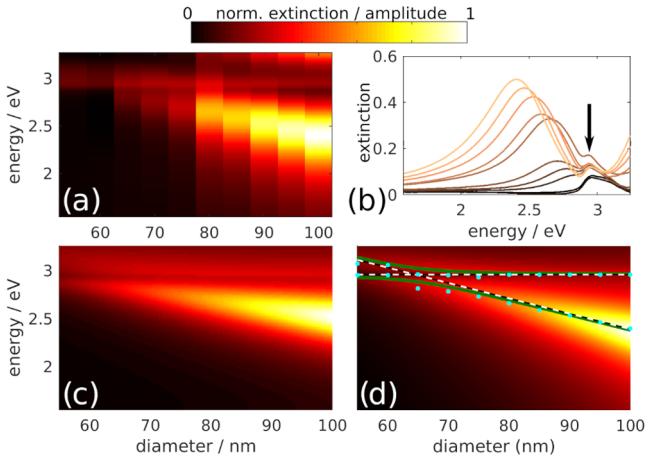

Figure 6. (a) Color map and (b) line plots of the experimental extinction spectra for SiO_2−AgI-covered nanodisk arrays with different particle diameters (compare Figure S8). The arrow in (b) indicates extinction due to uncoupled AgI. (c) Color map of the simulated extinction cross section, applying the quasistatic model. (d) Coupled oscillator model calculation showing the Al LSPR amplitude. The dashed black/white lines indicate the resonance energies of the two uncoupled oscillators. The green lines plot the resonance energies of the coupled oscillators. The cyan dots indicate the extinction maxima of the experimental spectra in (a), (b).

red-shifts and shows anticrossing at the AgI exciton line, indicative of coupling. The Al nanodisk extinction spectra for different disk diameters before and after covering with SiO_2 are shown in Figure S8 to illustrate the effect of SiO_2 in this system. The spectral width as exemplified for a 90 nm diameter disk is 370 meV, as shown in Figure S5b.

To simulate the observed spectral data, we apply a quasistatic description, modeling the Al nanodisks as oblate ellipsoids (closely approximating the disk shape) in a homogeneous environment with an effective permittivity derived from equal contributions from AgI, ITO, and SiO_2 to achieve the best fit. The polarizability of an ellipsoid in a homogeneous external field is given by

$$\alpha = \varepsilon_e V \frac{\varepsilon_m - \varepsilon_e}{\varepsilon_e + A(\varepsilon_m - \varepsilon_e)} \quad (2)$$

ε_e is the permittivity of the environment (AgI, see Figure 1b)), ε_m is the frequency-dependent metal (Al) permittivity,[20] V is the particle volume, and A is the ellipsoidal particle shape factor corresponding to the disk shape in the experiment. The extinction cross section $c_a \propto \Im(\alpha)$, where $\Im(\alpha)$ is the imaginary part of the polarizability, is plotted in Figure 6c. Despite the coarse model, the similarity between the model and the experiment is striking.

With this in mind, we model the experimentally observed spectral behavior by two coupled oscillators, similar to the model used for the Al−SiO_2−AgI film system. As light interaction and extinction are dominated by the LSPR, we plot in Figure 6d the oscillator amplitude only for the Al LSPR. Again, we find good accordance with the experimental results in Figure 6a and deduce an energy splitting of 100 meV. A closer view on the resonance region around 2.9 eV shows that in the experiment, some extinction is present within the anticrossing region, evident as the shoulder in the line spectra in Figure 6b, marked by the arrow. This is most likely due to some uncoupled AgI fraction, as to be expected from our sample geometry, compare with Figure 2.

CONCLUSIONS

Combining AgI and Al, we investigated the coupling of plasmons and excitons in the blue spectral range, demonstrating a large energy splitting of about 140 meV. We fabricated, on the one hand, a thin film stack involving surface plasmons and, on the other hand, nanodisks involving LSPRs, demonstrating the versatility of a fabrication scheme that simply relies on the iodization of silver. Overall, our results show that the coupling of AgI and Al plasmons can lead to the onset of strong coupling. It is thus to be expected that strong coupling can be achieved by optimizing the sample geometry and material parameters. For example, stronger coupling in Al−SiO_2−AgI systems is to be expected from increased AgI thickness or reduced SiO_2 thickness. In general, coupling AgI to Al plasmons provides a platform that could contribute to an increased control for nanoscale light/matter interaction, including applications in low-threshold lasers,[22] quantum information processing,[27] and single photon sources.[28]

ASSOCIATED CONTENT

Supporting Information

The Supporting Information is available free of charge at https://pubs.acs.org/doi/10.1021/acs.jpcc.0c09025.

Tauc plots of AgI; dielectric function of AgI; comparison of calculated and measured AgI absorbance spectra; SPR reflection spectra; resonance width of the Al surface plasmon; resonance width of AgI and the Al LSPR; energy splitting of the surface plasmon dispersion as a function of SiO_2 and AgI thickness; amplitudes as a function of energy and coupling constant of two coupled, damped oscillators; and extinction spectra of nanodisk arrays without and with SiO_2 layer (PDF)

AUTHOR INFORMATION

Corresponding Author

Razieh Talebi − *Faculty of Physics, University of Isfahan, 81746-73441 Isfahan, Iran; Quantum Optics Group, Faculty*

https://dx.doi.org/10.1021/acs.jpcc.0c09025
J. Phys. Chem. C XXXX, XXX, XXX−XXX

of Physics, University of Isfahan, 81746-73441 Isfahan, Iran; orcid.org/0000-0003-0209-2992; Email: r.talebi@sci.ui.ac.ir

Authors

Harald Ditlbacher − *Institute of Physics, University of Graz, 8010 Graz, Austria*

Joachim R. Krenn − *Faculty of Physics, University of Isfahan, 81746-73441 Isfahan, Iran; Quantum Optics Group, Faculty of Physics, University of Isfahan, 81746-73441 Isfahan, Iran; Institute of Physics, University of Graz, 8010 Graz, Austria*

Andreas Hohenau − *Institute of Physics, University of Graz, 8010 Graz, Austria;* orcid.org/0000-0002-9034-3044

Complete contact information is available at: https://pubs.acs.org/10.1021/acs.jpcc.0c09025

Author Contributions

J.R.K. and A.H. conceived the idea and supervised the project. R.T. introduced AgI for this project and fabricated all samples. A.H. and H.D. have participated in sample preparation. R.T. carried out the SPR spectroscopy in the Kretschmann−Raether configuration and performed all optical measurements. All calculations were performed by A.H after discussion with R.T., H.D., and J.R.K. The first manuscript was prepared by R.T. and edited and finalized by all authors. The final version of the figures was done by A.H.

Notes

The authors declare no competing financial interest.

■ ACKNOWLEDGMENTS

R.T. acknowledges partial financial support provided by the Austrian Academy of Science via Joint Excellence in Science and Humanities (JESH) program.

■ ABBREVIATIONS

AgI, silver iodide; Al, aluminum; ITO, indium tin oxide; LSPR, localized surface plasmon resonance; PMMA, poly(methyl methacrylate); SPR, surface plasmon resonance

■ REFERENCES

(1) Schlücker, S. Surface-enhanced Raman spectroscopy: Concepts and chemical applications. *Angew. Chem., Int. Ed.* **2014**, *53*, 4756−4795.

(2) Lozano, G.; Louwers, D. J.; Rodriguez, S. R. K.; Murai, S.; Jansen, O. T. A.; Verschuuren, M. A.; Rivas, J. G. Plasmonics for solid-state lighting: enhanced excitationand directional emission of highly efficient light sources. *Light Sci. Appl.* **2013**, *2*, No. e66.

(3) Schokker, A. H.; Koenderik, A. F. Statistics of randomized plasmonic lattice lasers. *ACS Photonics* **2015**, *2*, 1289−1297.

(4) Törmä, P.; Barnes, W. L. Strong coupling between surface plasmon polaritons and emitters: a review. *Rep. Prog. Phys.* **2015**, *78*, No. 013901.

(5) Pelton, M.; Storm, S. D.; Leng, H. Strong coupling of emitters to single plasmonic nanoparticles: exciton-induced transparency and Rabi splitting. *Nanoscale* **2019**, *11*, 14540−14552.

(6) Bellessa, J.; Bonnand, C.; Plenet, J. C. Strong coupling between surface plasmons and excitons in an organic semiconductor. *Phys. Rev. Lett.* **2004**, *93*, No. 036404(1).

(7) Hakala, T. K.; Toppari, J. J.; Kuzyk, A.; Pettersson, M.; Tikkanen, H.; Kunttu, H.; Törmä, P. Vacuum Rabi splitting and strong coupling dynamics for surface plasmon polaritons and Rhodamine 6G molecules. *Phys. Rev. Lett.* **2009**, *103*, No. 053602(1).

(8) Santhosh, K.; Bitton, O.; Chuntonov, L.; Haran, G. Vacuum Rabi splitting in a plasmonic cavity at the single quantum emitter limit. *Nat. Commun.* **2016**, *7*, No. 11823.

(9) Shlesinger, I.; Monin, H.; Moreau, J.; Hugonnin, J. P.; Dufour, M.; Ithurria, S.; Vest, B.; Greffet, J. J. Strong coupling of nanoplatelets and surface plasmons on a gold surface. *ACS Photonics* **2019**, *6*, 2643−2648.

(10) Lawrie, B. J.; Kim, K. W.; Norton, D. P.; Haglund, R. F., Jr Plasmon−Exciton hybridization in ZnO quantum-well Al nanodisc heterostructures. *Nano Lett.* **2012**, *12*, 6152−6157.

(11) Knight, M. W.; King, N. S.; Liu, L.; Everitt, H. O.; Nordlander, P.; Halas, N. J. Aluminum for plasmonics. *Nano Lett.* **2014**, *8*, 834−840.

(12) Burley, G. Photolytic behavior of silver iodide. *J. Res. Natl. Bur. Stand., Sect. A* **1963**, *67*, 301−307.

(13) Mohan, D. B.; Sreejith, K.; Sunandana, C. S. Surface plasmon−exciton transition in ultra-thin silver and silver iodide films. *Appl. Phys. B* **2007**, *89*, 59−63.

(14) Andreeva, O. V.; Sidorov, A. I.; Stasel'ko, D. I.; Khrushcheva, T. A. Synthesis and Optical Properties of Hybrid "Plasmon−Exciton" Nanostructures Based on Ag−AgI in Nanoporous Silica Glass. *Phys. Solid State* **2012**, *54*, 1293−1297.

(15) El-Kouedi, M.; Foss, C. A. Optical Properties of Gold-Silver Iodide Nanoparticle Pair Structures. *J. Phys. Chem. B* **2000**, *104*, 4031−4037.

(16) Bashouti, M. Y.; Talebi, R.; Kasar, T.; Nahal, A.; Ristein, J.; Unruh, T.; Christiansen, S. H. Systematic Surface Phase Transition of Ag Thin Films by Iodine Functionalization at Room Temperature: Evolution of Optoelectronic and Texture Properties. *Sci. Rep.* **2016**, *6*, No. 21439.

(17) Kumar, P. S.; Dayal, P. B.; Sunandana, C. S. On the formation mechanism of γ-AgI thin films. *Thin Solid Films* **1999**, *357*, 111−118.

(18) Cochrane, G. Some optical properties of single crystals of hexagonal silver iodide. *J. Phys. D: Appl. Phys.* **1974**, *7*, 748−758.

(19) Ono, A.; Kikawada, M.; Akimoto, R.; Inami, W.; Kawata, Y. Fluorescence enhancement with deep-ultraviolet surface plasmon excitation. *Opt. Express* **2013**, *21*, 17447−17453.

(20) McPeak, K. M.; Jayanti, S. V.; Kress, S. J. P.; Meyer, S.; Iotti, S.; Rossinelli, A.; Norris, D. J. Plasmonic films can easily be better: Rules and recipes. *ACS Photonics* **2015**, *2*, 326−333.

(21) Symonds, C.; Bonnand, C.; Plenet, J. C.; Bréhier, A.; Parashkov, R.; Lauret, J. S.; Deleporte, E.; Bellessa, J. Particularities of surface plasmon−exciton strong coupling with large Rabi splitting. *New J. Phys.* **2008**, *10*, No. 065017(1).

(22) Hakala, T. K.; Rekola, H. T.; Väkeväinen, A. I.; Martikainen, J.-P.; Necada, M.; Moilanen, A. J.; Törmä, P. Lasing in dark and bright modes of a finite-sized plasmonic lattice. *Nat. Commun.* **2012**, *86*, No. 13687.

(23) Novotny, L. Strong coupling, energy splitting, and level crossing: A classical perspective. *Am. J. Phys.* **2017**, *8*, 1199−1202.

(24) Gómez, D. E.; Lo, S. S.; Davis, T. J.; Hartland, G. V. Picosecond Kinetics of Strongly Coupled Excitons and Surface Plasmon Polaritons. *J. Phys. Chem. B* **2013**, *117*, 4340−4346.

(25) Zengin, G.; Gschneidtner, T.; Verre, R.; Shao, L.; Antosiewicz, T. J.; Moth-Poulsen, K.; Käll, M.; Shegai, T. Evaluating conditions for strong coupling between nanoparticle plasmons and organic dyes using scattering and absorption spectroscopy. *J. Phys. Chem. C* **2016**, *120*, 20588−20596.

(26) Antosiewicz, T. J.; Apell, S. P.; Shegai, T. Plasmon-exciton interactions in a core-shell-geometry: From enhanced absorption to strong coupling. *ACS Photonics* **2014**, *1*, 454−463.

(27) Hennessy, K.; Badolato, A.; Winger, M.; Gerace, D.; Atatre, M.; Gulde, S.; Flt, S.; Hu, E. L.; Imamoglu, A. Quantum nature of a strongly coupled single quantum dot-cavity system. *Nature* **2007**, *445*, 896−899.

(28) Cui, G.; Raymer, M. G. Quantum efficiency of single-photon sources in the cavity-QED strong-coupling regime. *Opt. Express* **2005**, *13*, 9660−9665.